GEOLOGY

Troughs developed in ice-stream shear margins precondition ice shelves for ocean-driven breakup

Karen E. Alley[1,2]*, Ted A. Scambos[2], Richard B. Alley[3], Nicholas Holschuh[4]

Floating ice shelves of fast-flowing ice streams are prone to rift initiation and calving originating along zones of rapid shearing at their margins. Predicting future ice-shelf destabilization under a warming ocean scenario, with the resultant reduced buttressing, faster ice flow, and sea-level rise, therefore requires an understanding of the processes that thin and weaken these shear margins. Here, we use satellite data to show that high velocity gradients result in surface troughs along the margins of fast-flowing ice streams. These troughs are advected into ice-shelf margins, where the locally thinned ice floats upward to form basal troughs. Buoyant plumes of warm ocean water beneath ice shelves can be focused into these basal troughs, localizing melting and weakening the ice-shelf margins. This implies that major ice sheet drainages are preconditioned for rapid retreat in response to ocean warming.

INTRODUCTION

More than 80% of Antarctica's ice flux into the Southern Ocean passes through the continent's ice shelves (*1*). These floating extensions of the ice sheet play a key role in regulating rates of grounded ice flow into the ocean, which is a fundamental control on sea-level rise. Ice shelves hold back grounded ice through the upstream transmission of stresses from shearing along ice-shelf margins and against basal pinning points (*2*–*4*). The loss of buttressing due to ice-shelf thinning or collapse leads to acceleration of grounded ice (*5*, *6*); in particular, loss of buttressing at ice-shelf shear margins has far-reaching consequences for the mass balance of the Antarctic Ice Sheet (*6*).

Antarctica's ice shelves are, on average, losing mass at accelerating rates (*1*, *7*), primarily due to faster basal melting (*8*). This acceleration is most pronounced around the Amundsen and Bellingshausen Seas regions, where warm Circumpolar Deep Water (CDW) intrudes onto the continental shelf (*9*). CDW transport in sub–ice-shelf cavities is a complex function of tidal forces, Coriolis forces, and buoyant flows driven by melting ice shelves or subglacial discharge (*10*). These forces, on average, lead to melting that is focused in the deepest and rotationally favored (left for southern hemisphere and right for northern hemisphere) portions of the ice shelf (*11*, *12*). Both large- and small-scale features of the cavity shape, however, can exert primary control on heat-transport dynamics, with buoyant meltwater plumes contributing to the development of sub–ice-shelf channels where ice is locally thinned (*13*).

While observations have shown preferred melting on the sub–ice-shelf keels in some cases (*14*) and within channels in others (*15*, *16*), sub–ice-shelf channels have been shown to reduce the direct impact of ocean warming by localizing melt and lowering shelf-averaged melt rates (*10*, *17*), which reduces the loss of ice-shelf buttressing and grounding-line retreat observed around Antarctica (*6*, *8*). Indirectly, however, channelized melting may exert additional effects through localized mechanical weakening, which allows for enhanced fracturing and more frequent calving events, promoting loss of buttressing and retreat (*18*–*20*). Basal channels can and do exist in steady-state ice shelves. However, the presence of increased amounts of warm water encourages the formation and deepening of large basal channels (*10*), which may trigger faster ice-shelf flow and calving through this mechanical weakening. This implies that warmer conditions in the future may increase ice-shelf retreat and sea-level rise through basal channel formation and deepening.

[1]Department of Earth Sciences, College of Wooster, Wooster, OH 44691, USA. [2]Cooperative Institute for Research in Environmental Sciences (CIRES), University of Colorado Boulder, Boulder, CO 80309, USA. [3]Department of Geosciences, Penn State University, State College, PA 16802, USA. [4]Department of Earth and Space Sciences, University of Washington, Seattle, WA 98195, USA.
*Corresponding author. Email: kalley@wooster.edu

RESULTS AND DISCUSSION

Ice-shelf shear margins and calving

Strain rates and stresses are especially high in ice-shelf shear margins, frequently exceeding the physical thresholds for major fracturing (*21*). Rifts originating in shear margins often propagate into fast moving, more strongly extensional ice in central regions of ice shelves, eventually joining with rifts from opposite shear margins or reaching opposite shear margins, triggering calving. This pattern can be part of steady-state ice flow and calving behavior, or it can be a component of non–steady-state retreat. Through this mechanism, processes that contribute to shear margin weakening increase the likelihood of shear margin fracture, which may increase rates of calving and promote retreat under warming conditions.

Two examples of this shear margin rift propagation are shown in Fig. 1. Pine Island Glacier (PIG) in Antarctica (Fig. 1A) experienced a large calving event in 2007 caused by rift propagation from both shear margins. Similarly, a single fracture propagating across the ice shelf from the right-lateral shear margin initiated a large calving event on Petermann Glacier in Greenland in 2010 (Fig. 1B). Note that PIG experienced localized retreat along its weak, fractured shear margins preceding the calving event. Ocean-induced retreat of Jakobshavn Isbræ exhibited the same behavior during the early 2000s, when extensive shear margin fracturing and shear margin retreat preceded the catastrophic loss of mid-shelf ice (movie S1). More examples of the common patterns of shear margin fracture and retreat can be seen in figs. S1 to S6. These example ice shelves have diverse characteristics, including widely varying basal melt and thinning rates, geometries, and grounding-line depths (table S1), but they all have zones of relatively high shear strain rates along their margins where calving and retreat are initiated. Furthermore, some of these examples, including PIG and Petermann, have mapped basal channels beneath their shear margins (*18*, *22*).

Evidence for basal channels beneath shear margins

Identifying basal channels beneath shear margins is complicated by their inaccessibility and complex surface topography. Past studies (*20*, *22*, *23*)

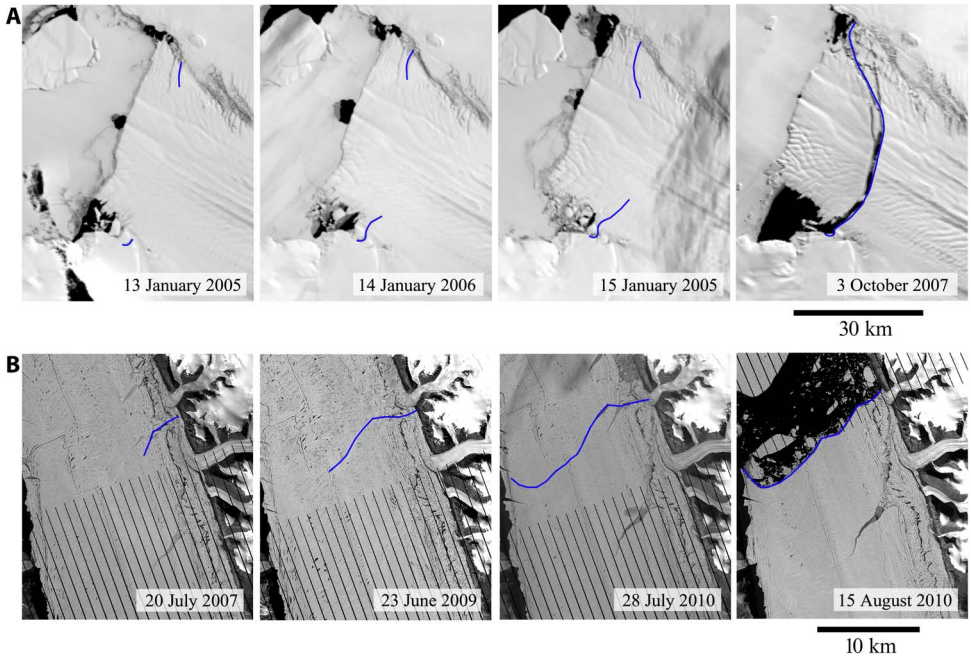

Fig. 1. Major calving events initiated by shear margin fractures. Blue lines trace the fractures that led directly to a major calving event. (**A**) PIG from the Moderate Resolution Imaging Spectroradiometer (MODIS) Ice Shelf Image Archive (*27*). (**B**) Petermann Glacier from a series of Landsat 7 images.

have identified basal channels by proxy, inferring their presence using linear depressions on the ice-shelf surface, which form as the ice shelf adjusts to hydrostatic equilibrium over channels. However, in highly crevassed shear margins, complex surfaces make visual identification of channels from surface features unreliable. Similarly, ice-penetrating radar has been used to identify channels in ice-shelf bases (*22*, *24*), but radar is difficult to collect and interpret in heavily crevassed shear margins.

Basal channels have also been identified by tracking the presence of persistent polynyas at the ice-shelf edge (*22*, *25*, *26*). We define persistent polynyas as small, open-water areas at the ice-shelf front, visible when fast ice is present, that are located in the same spot relative to the ice-shelf edge in at least three seasons. Here, we expand work begun in (*22*) using the Moderate Resolution Imaging Spectroradiometer (MODIS) Ice Shelf Image Archive (*27*) to map and track the presence of persistent polynyas through time (Fig. 2, movies S2 to S13, and fig. S7). Thirty-three persistent polynyas were identifiable in the image archive; example polynyas are shown in Fig. 2 (B to D) for three ice shelves in the Amundsen Sea. Each of these example polynyas forms at the terminus of a shear margin, which experiences relatively high shear strain rates (shown in red). Of the 33 polynyas tracked, 18 correspond directly to a shear margin.

Persistent formation of polynyas at an ice-shelf front implies consistent interactions between the ice-shelf front, fast ice, and/or sub–ice shelf circulation. Wind stress can create open-water areas at the ice shelf front by pushing the sea ice away from the coastline, but this forms linear leads, rather than the relatively circular polynyas mapped. Similarly, the advance of the ice-shelf front may drag fast ice out to sea, potentially leaving open-water areas in notches where shear margins have retreated. However, the polynyas observed in this study frequently protrude seaward into fast ice. This suggests that mechanical movement of the fast ice due to ice-shelf front advance cannot fully explain polynya formation, although it might contribute to weakening of fast ice in those areas. In addition, we observe these polynyas to open at much faster rates than ice front advances (movies S2 to S13). More likely, the polynyas we observe outboard of shear margins result from the localized flow of warm, buoyant water along a basal channel, which prevents the formation of fast ice at the ice-shelf front (*25*, *26*).

The consistent locations of these polynyas are likely the result of consistent delivery of buoyant water to the ice shelf edge, which has been shown to occur as the result of channelization on the underside of the ice shelf (*25*, *26*). Therefore, the presence of a shear margin–associated persistent polynya is likely to be evidence of a shear margin basal channel. In addition, it is likely that some shear margins have basal channels, although they do not have persistent polynyas; channels can occur without polynyas for many reasons, including lack of fast ice, lack of sufficient amounts of warm water, and along-flow flattening of the ice shelf base, which reduces plume flow velocity and warm-water entrainment. Notably, we find basal channels beneath shear margins on all three major ice shelves in Pine Island Bay and on several other ice shelves in the Amundsen and Bellingshausen Seas regions where CDW is consistently observed (*28*).

Oceanic influences on basal channel formation in shear margins

There are several reasons that basal channels may preferentially form in shear margins, which we review briefly here before arguing that processes on grounded ice are typically most important. The Coriolis force can cause overturning ocean circulation in ice shelf cavities to exit as a plume on the left-hand (right-hand) side of the cavity in the Southern (Northern) Hemisphere (*29*), which may promote channelized melt regardless of an ice shelf's basal topography. However, some persistent polynyas, such as those on PIG (Fig. 2B and movie S2) and Thwaites Glacier (movie S3), are found on the opposite side of the cavity; therefore, the Coriolis effect cannot fully explain the collocation of shear margins and basal channels.

Basal channels form where buoyant water is concentrated, and buoyant water concentrates in local high spots of the ice shelf base. Therefore,

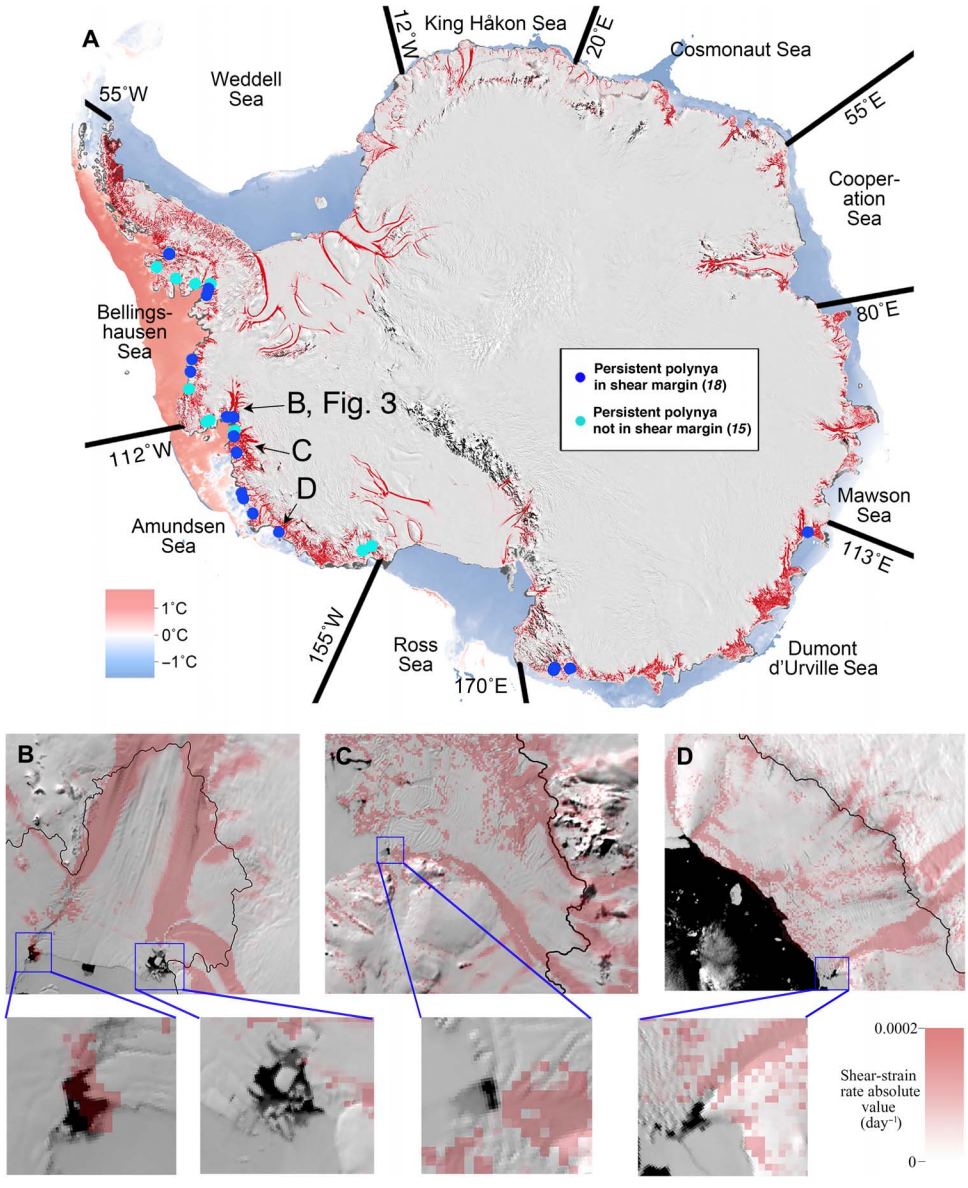

Fig. 2. Locations and examples of persistent polynyas. (**A**) Dots show polynyas at shear margins (blue) and outside shear margins (cyan). Background image is the 2009 MODIS Mosaic of Antarctica [MOA, (*37*)]. Locations are shown in insets (**B**) to (**D**). Ocean-bottom temperatures are from (*28*). Shear strain rates shown in red are from (*38*). Figure modified from (*22*). (B) PIG. Note that polynyas are present in both shear margins, along with a mid-shelf polynya at the terminus of a basal channel that formed outside a shear margin. (C) Crosson Ice Shelf. (D) Getz Ice Shelf. (B to D) images are from (*27*). Zoomed-in insets are shown for each polynya at the end of a shear margin. Grounding lines from (*37*) are shown in black.

any process that leads to locally thin ice will contribute to the formation of basal channels. For example, strain heating sufficient to cause melting could thin ice (*30*), although sufficiently high strain rates occur in few places in Antarctica (*31*) and ice flow through shear margins generally cools them sufficiently to avoid rapid melting (*32*). In addition, many fast-flowing ice streams exit the ice sheet through large bedrock troughs, so the floating ice shelf is thinner on the edges and subglacial plumes may be routed around the thick, central region. However, the abundance of mid-shelf, ocean-sourced basal channels (*22*) demonstrates that local high spots in the ice shelf base play a more important role in basal channel location than large-scale patterns of ice shelf thickness.

Grounded ice influences on basal channel formation in shear margins

These considerations, plus observations summarized next, indicate that ice dynamic processes on grounded ice streams are especially important in generating the local high spots in the ice-shelf base that are collocated with ice shelf shear margins. Where grounded ice flows across shear margins laterally from adjacent slow-moving areas into ice streams, it turns sharply downstream while undergoing rapid acceleration that causes stretching and thinning. Ice toward the ice-stream center either entered the head of the ice stream from the catchment without crossing a shear margin or crossed the shear margin farther upstream where ice is typically thicker. The result is a trough in surface elevation along the

shear margin. We diagram this process in Fig. 3A. These grounded shear margin troughs have been documented in Greenland (*33*, *34*); here, we use the Reference Elevation Model of Antarctica (*35*) to show that these troughs are also present in ice streams across Antarctica. Figure 3 (B to D) shows an example of large troughs in the grounded shear margins of PIG. The trough geometry closely correlates with high shear strain rates (Fig. 3C). We have provided 10 more examples of grounded shear margin troughs in ice streams distributed around Antarctica in figs. S2 to S6 and S8 to S12. Unless subglacial topography, such as the presence of mountains, substantially disrupts a shear margin, these troughs can be observed with varying magnitudes at any ice stream with high shear strain rates in its margins.

The surface troughs in grounded shear margins are continuous across the grounding line, becoming local high spots in ice shelf bases that promote basal channel formation in floating shear margins. Figure 4 shows the right-lateral shear margin trough at PIG (location marked in Fig. 3B) from grounded ice to floating ice. Three elevation transects reveal a continuous surface trough (Fig. 4, B to E), which is approximately 80-m-deep upstream of the grounding line (Fig. 4B). This trough shallows in going from grounded to floating ice due to hydrostatic adjustment (Fig. 4D). However, the trough is significantly deeper on the surface and extends higher into the base of the shelf (Fig. 4E; basal elevation predicted on the basis of hydrostatic equilibrium; see Materials and Methods) than it should be based on the geometry of the grounded trough alone. This implies that a channelized warm-water plume, which has been observed to terminate in a persistent polynya at the end of this shear margin (*25*, *26*), is likely responsible for thinning the ice shelf by incising a basal channel beneath the seaward extension of the grounded shear margin trough. This localized thinning does not necessarily imply non–steady-state ice shelf thickness change, but the presence of the thin band of ice does require high steady-state basal melt rates, at least near the grounding line.

Steep slopes near the grounding line make the trough difficult to identify in Fig. 4F; therefore, in Fig. 4G, we have normalized the surface elevations along transects perpendicular to the shear margin, so that the low point is at the center of the trough (see Materials and Methods). This normalization reveals that the trough is laterally continuous from grounded to floating ice, strongly suggesting that the grounded shear margin trough provided the local high spot in the ice shelf base that became the floating shear margin basal channel.

Shear margin troughs that are laterally continuous from grounded to floating ice are present in many shear margins throughout Antarctica; we have given 10 more examples in figs. S13 to S22. We selected these example shelves to show that shear margin troughs create channels on floating ice shelves with widely varying locations, geometries, and mass balance characteristics (table S1). On relatively small shelves where warm water is present, these channels are likely to carry substantial volumes of warm water that reach the ice shelf edge, sometimes forming polynyas (e.g., Getz Ice Shelf and Crosson Ice Shelf). On larger shelves in colder water, buoyant plumes may incise up-glacier but then supercool and refreeze before reaching the ice shelf edge [e.g., Amery Ice Shelf and Ronne Ice Shelf; (*36*)]. In the absence of high shear strain rates on the ice shelf, the locally thinned areas will infill through viscous creep processes (e.g., Ross Ice Shelf). The presence of grounded shear margin troughs that advect onto floating ice, therefore, does not imply that there must be a substantial amount of warm water flowing along the resultant thin zone; rather, if warm water is present and plume dynamics dominate the system, then the existence of shear margin troughs makes it more likely that the warm water will be focused along already-weak floating shear margins.

CONCLUSIONS

The frequent presence of polynyas collocated with shear margins suggests that warm water likely preferentially channelizes in troughs initiated by processes in the grounded ice. The localized thinning and mechanical weakening caused by basal channels increase the likelihood that fracture and rifting initiate in these already-weak zones. Because these troughs form most prominently at the shear margins of fast-flowing ice streams, where velocity gradients are high, and because ice shelves have been observed to retreat in association with shear margin–originating fractures, these observations strongly imply that the floating ice shelves of fast-flowing ice streams have a greater tendency toward ocean-induced instability than the floating ice shelves of slower-flowing ice streams, which have smaller velocity gradients at their margins and therefore are less likely to develop prominent shear margin troughs.

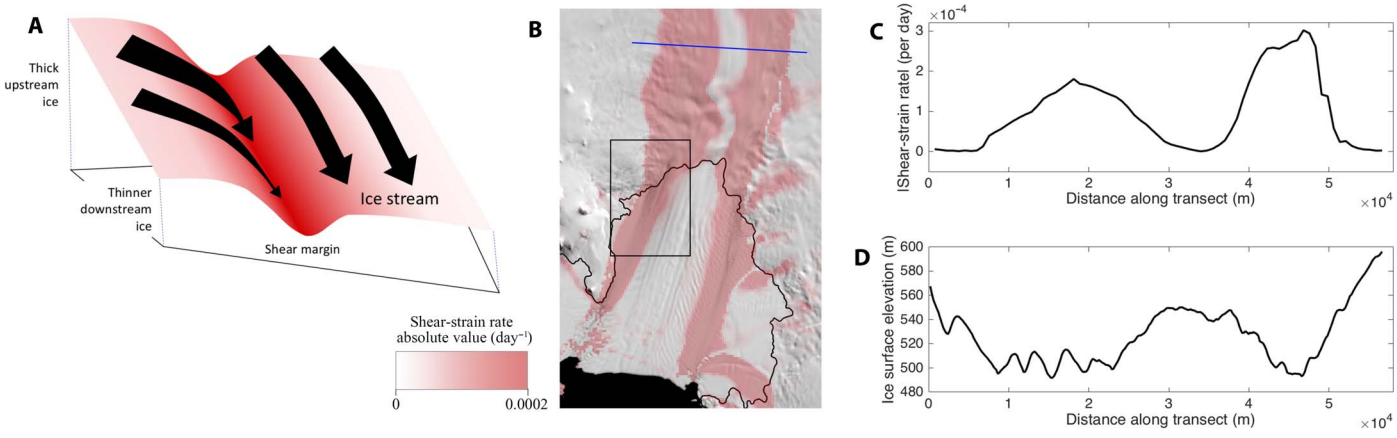

Fig. 3. The formation of grounded shear margin troughs. (**A**) Diagram of the dynamic contributions to shear margin trough formation. (**B**) PIG ice stream and ice shelf, with background and grounding line from (*37*) and shear strain rates from (*38*). The blue line is the transect shown in (**C** to **E**). The black box is the area shown in Fig. 4A. (D) Absolute value of the surface shear strain rates across both grounded shear margins of PIG from (*38*). (E) Surface ice elevations across both grounded shear margins of PIG from (*35*).

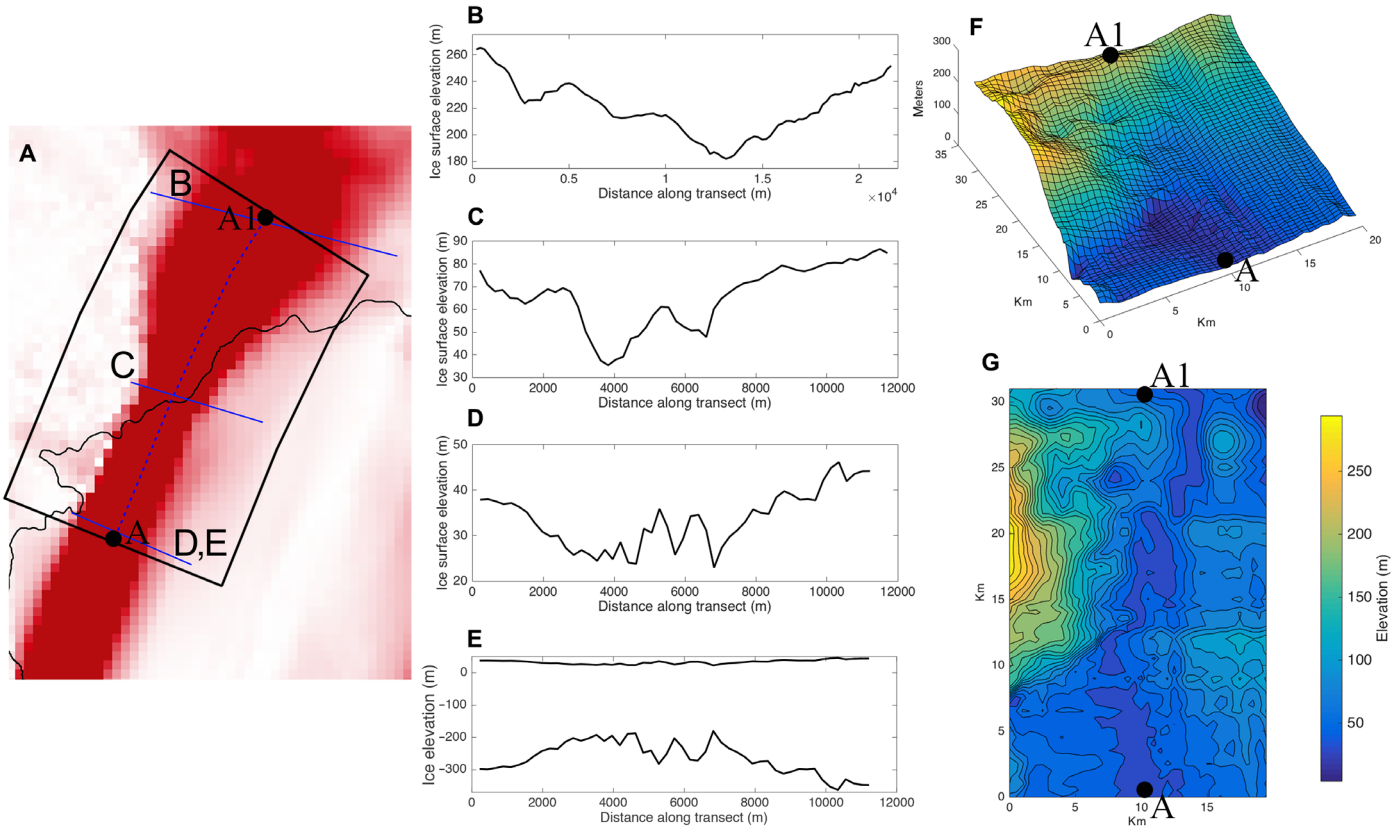

Fig. 4. Continuous trough from grounded to floating ice in the right-lateral shear margin of PIG. (**A**) Location indicated in Fig. 3B. Shear strain rates in red from (*38*). Blue lines are transects shown in (**B**) to (**E**). Black box outlines area shown in (E) and (F). Grounding line from (*37*). (B to D) Ice surface elevations from (*35*) showing troughs above, at, and below the grounding line. Note different elevation scales in (B) to (D) as trough adjusts to hydrostatic equilibrium. (E) Same transect as (D) but with basal channel topography beneath the shelf is also shown (see Materials and Methods). (F) Topography from the black outline shown in (A). (G) Contour map of topography shown in (E), with elevation slices normalized to the trough-bottom height (see Materials and Methods).

Because shear margin troughs tend to localize basal meltwater beneath both grounded and floating ice, their widespread occurrence has many implications for ice sheet and ice shelf behavior. For example, the stability and migration of grounded shear margins are influenced by the distribution of subglacial lubrication (*32*), and the formation of ice shelves during times of cooling and ice advance in the past must has been made more difficult by the presence of basal channels reducing resistive back stress and buttressing in shear margins. Critically, in our modern warming climate, warming of sub–ice shelf water may already be causing basal channel deepening in shear margins (*22*), which could strongly affect buttressing and may lead to enhanced calving and ice mass loss. Further analysis is needed to establish the current and likely future behavior of shear margin troughs and basal channels, and models of ice sheet change should incorporate the impacts of preferentially weakened shear margins in both paleo and modern simulations.

MATERIALS AND METHODS

Trough mapping through elevation normalization

Figure 4 and figs. S2 to S6 and S8 to S12 used normalized surface elevations to reveal the continuous nature of troughs from grounded to floating ice in shear margins. These troughs are identifiable in surface elevation transects perpendicular to the shear margins (Figs. 3, C and D, and 4, B to Dand figs. S2 to S6 and S8 to S12), but they are difficult to represent in continuous, gridded views of shear margin elevations due to the strong elevation gradients present near grounding lines. Removing the background trend makes the troughs apparent.

To remove the background trend, we selected a grounding line region with high shear strain rates and drew a trace (blue dashed lines in Fig. 4A) along the approximate center of the shear margin, according to the shear strain rates. It is unlikely that troughs will follow the center of the shear margins precisely, due to complex shear margin flow as well as differential accumulation and firn densification (*34*). Therefore, we generated elevation profiles perpendicular to the trace (figs. S2 to S6A and S8 to S12A) that were long enough to span the entire shear margin, ensuring that the shear margin trough was included somewhere in each profile.

We extracted elevations along the perpendicular profiles and used these to recreate the original topography, which is shown in Fig. 4F and figs. S2 to S6E and S8 to S12E. There are two important advantages to using these perpendicular profiles to represent the topography: (i) Plotting the profiles on a regular grid effectively straightens the shear margins so that they are approximately parallel to the edges of the grid; and (ii) because troughs are expected to be approximately parallel to shear margins, topography normalization will most clearly reveal troughs if it is applied to slices that are perpendicular to the trough, so that none of the cross-trough trend is removed from the data.

We selected the point with the minimum elevation in the central half of each perpendicular transect. This point was assumed to be the

bottom of a shear margin trough. Each perpendicular transect was then adjusted linearly up or down so that the new trough bottom points all aligned at the mean trough bottom elevation. The resulting gridded and normalized elevation plots are shown in Fig. 4G and figs. S2 to S6F and S8 to S12F. If the plot showed that the trough bottom lay outside the central half of each perpendicular transect, then we reran the code to select the minimum value in the first or second half of each perpendicular transect. At no time did we manually dictate the exact locations of the trough bottoms.

Calculation of ice shelf base using hydrostatic equilibrium

In Fig. 4D, we showed the surface elevation of the ice shelf from (*32*) and the basal elevation calculated on the basis of the hydrostatic relationship between ice thickness and surface elevation, using the following equation

$$Z_s = \left(1 - \frac{\rho_i}{\rho_w}\right) H$$

where z_s is the surface elevation, ρ_i is the density of ice (we assumed a value of 910 kg/m^3), ρ_w is the density of seawater (we assumed a value of 1024 kg/m^3), and H is the ice thickness.

SUPPLEMENTARY MATERIALS

Supplementary material for this article is available at http://advances.sciencemag.org/cgi/content/full/5/10/eaax2215/DC1

Fig. S1. Locations of figs. S2 to 6 and S8 to S12.
Fig. S2. Troughs and fracture in the shear margins of the Jutulstraumen Glacier and Fimbul Ice Shelf.
Fig. S3. Troughs and fracture in the shear margins of the Rayner Glacier and Ice Shelf.
Fig. S4. Troughs and fracture in the shear margins of the Denman Glacier and Shackleton Ice Shelf.
Fig. S5. Troughs and fracture in the shear margins of the Ninnis Glacier and Ice Shelf.
Fig. S6. Troughs and fracture in the shear margins of the PIG and Ice Shelf.
Fig. S7. Observations for all 33 identified persistent polynyas.
Fig. S8. Trough in the left-lateral shear margin of the Fisher Glacier and Amery Ice Shelf.
Fig. S9. Troughs in the shear margins of the Byrd Glacier and Ross Ice Shelf.
Fig. S10. Trough in the shear margins of the Bindschadler Ice Stream and Ross Ice Shelf.
Fig. S11. Trough in the left-lateral shear margin of the Evans Ice Stream and Ronne Ice Shelf.
Fig. S12. Trough in the right-lateral shear margin of the Slessor Ice Stream and Filchner Ice Shelf.
Table S1. Comparison of characteristics of ice shelves with observed continuous shear margin troughs from grounded to floating ice in figs. S2 to S6 and S8 to S22.
Movie S1. Calving and collapse of Jakobshavn Isbrae.
Movie S2. Persistent polynyas on PIG.
Movie S3. Persistent polynyas on Thwaites Glacier.
Movie S4. Persistent polynyas on the Crosson Ice Shelf.
Movie S5. Persistent polynyas on Eastern Getz Ice Shelf.
Movie S6. Persistent polynyas on the Western Getz Ice Shelf (DeVicq Glacier).
Movie S7. Persistent polynyas on the Sulzberger Ice Shelf.
Movie S8. Persistent polynyas on the Lillie and Rennick Ice Shelves.
Movie S9. Persistent polynyas on Totten Glacier.
Movie S10. Persistent polynyas on the northern George VI and Wilkins Ice Shelves.
Movie S11. Persistent polynyas on the southern George VI and Bach Ice Shelves.
Movie S12. Persistent polynyas on the Venable and Abbot Ice Shelve.
Movie S13. Persistent polynyas on the Cosgrove Ice Shelf.

REFERENCES AND NOTES

1. E. Rignot, S. Jacobs, J. Mouginot, B. Scheuchl, Ice-shelf melting around Antarctica. *Science* **341**, 266–270 (2013).
2. R. H. Thomas, D. R. MacAyeal, Derived characteristics of the ross ice shelf, Antarctica. *J. Glaciol.* **28**, 397–412 (1982).
3. T. K. Dupont, R. B. Alley, Assessment of the importance of ice-shelf buttressing to ice-sheet flow. *Geophys. Res. Lett.* **32**, L04503 (2005).
4. J. J. Fürst, G. Durand, F. Gillet-Chaulet, L. Tavard, M. Rankl, M. Braun, O. Gagliardini, The safety band of Antarctic ice shelves. *Nat. Clim. Chang.* **6**, 479–482 (2016).
5. T. A. Scambos, J. Bohlander, C. A. Shuman, P. Skvarca, Glacier acceleration and thinning after ice shelf collapse in the Larsen B embayment Antarctica. *Geophys. Res. Lett.* **31**, L18402–4 (2004).
6. R. Reese, G. H. Gudmundsson, A. Levermann, R. Winkelmann, The far reach of ice-shelf thinning in Antarctica. *Nat. Clim. Chang.* **8**, 53–57 (2017).
7. F. S. Paolo, H. A. Fricker, L. Padman, Volume loss from Antarctic ice shelves is accelerating. *Science* **348**, 327–331 (2015).
8. H. D. Pritchard, S. R. M. Ligtenberg, H. A. Fricker, D. G. Vaughan, M. R. van den Broeke, L. Padman, Antarctic ice-sheet loss driven by basal melting of ice shelves. *Nature* **484**, 502–505 (2012).
9. S. Jacobs, A. Jenkins, H. Hellmer, C. Giulivi, F. Nitsche, B. Huber, R. Guerrero, The Amundsen Sea and the Antarctic Ice Sheet. *Oceanography* **25**, 154–163 (2012).
10. C. V. Gladish, D. M. Holland, P. R. Holland, S. F. Price, Ice-shelf basal channels in a coupled ice/ocean model. *J. Glaciol.* **58**, 1227–1244 (2012).
11. S. S. Jacobs, A. Jenkins, C. F. Giulivi, P. Dutrieux, Stronger ocean circulation and increased melting under Pine Island Glacier ice shelf. *Nat. Geosci.* **4**, 519–523 (2011).
12. J. R. Jordan, P. R. Holland, D. Goldberg, K. Snow, R. Arthern, J.-M. Campin, P. Heimbach, A. Jenkins, Ocean-forced ice-shelf thinning in a synchronously coupled ice-ocean model. *J. Geophys. Res.* **123**, 864–882 (2018).
13. O. V. Sergienko, Basal channels on ice shelves. *J. Geophys. Res.* **118**, 1342–1355 (2013).
14. C. Cai, E. Rignot, D. Menemenlis, Y. Nakayama, Observations and modeling of ocean-induced melt beneath Petermann Glacier Ice Shelf in northwestern Greenland. *Geophys. Res. Lett.* **44**, 8396–8403 (2017).
15. T. P. Stanton, W. J. Shaw, M. Truffer, H. F. J. Corr, L. E. Peters, K. L. Riverman, R. Bindschadler, D. M. Holland, S. Anandakrishnan, Channelized ice melting in the ocean boundary layer beneath Pine Island Glacier, Antarctica. *Science* **341**, 1236–1239 (2013).
16. O. J. Marsh, H. A. Fricker, M. R. Siegfried, K. Christianson, K. W. Nicholls, H. F. J. Corr, G. Catania, High basal melting forming a channel at the grounding line of Ross Ice Shelf, Antarctica. *Geophys. Res. Lett.* **43**, 250–255 (2016).
17. T. Millgate, P. R. Holland, A. Jenkins, H. L. Johnson, The effect of basal channels on oceanic ice-shelf melting. *J. Geophys. Res.* **118**, 6951–6964 (2013).
18. E. Rignot, K. Steffen, Channelized bottom melting and stability of floating ice shelves. *Geophys. Res. Lett.* **35**, L02503 (2008).
19. D. G. Vaughan, Relating the occurrence of crevasses to surface strain rates. *J. Glaciol.* **39**, 255–266 (1993).
20. C. F. Dow, W. S. Lee, J. S. Greenbaum, C. A. Greene, D. D. Blankenship, K. Poinar, A. L. Forrest, D. A. Young, C. J. Zappa, Basal channels drive active surface hydrology and transverse ice shelf fracture. *Sci. Adv.* **4**, eaao7212 (2018).
21. E. M. Schulson, Brittle failure of ice. *Eng. Fract. Mech.* **68**, 1839–1887 (2001).
22. K. E. Alley, T. A. Scambos, M. R. Siegfried, H. A. Fricker, Impacts of warm water on Antarctic ice shelf stability through basal channel formation. *Nat. Geosci.* **9**, 290–293 (2016).
23. R. Drews, Evolution of ice-shelf channels in Antarctic ice shelves. *Cryosphere* **9**, 1169–1181 (2015).
24. K. Langley, A. von Deschwanden, J. Kohler, A. Sinisalo, K. Matsuoka, T. Hattermann, A. Humbert, O. A. Nøst, E. Isaksson, Complex network of channels beneath an Antarctic ice shelf. *Geophys. Res. Lett.* **41**, 1209–1215 (2014).
25. R. Bindschadler, D. G. Vaughan, P. Vornberger, Variability of basal melt beneath the Pine Island Glacier ice shelf, West Antarctica. *J. Glaciol.* **57**, 581–595 (2011).
26. K. D. Mankoff, S. S. Jacobs, S. M. Tulaczyk, S. E. Stammerjohn, The role of Pine Island Glacier ice shelf basal channels in deep-water upwelling, polynyas and ocean circulation in Pine Island Bay, Antarctica. *Ann. Glaciol.* **53**, 123–128 (2012).
27. T. A. Scambos, J. Bohlander, B. Raup, *Images of Antarctic Ice Shelves* (National Snow and Ice Data Center, Boulder, CO, USA, 1996).
28. S. Schmidtko, K. J. Heywood, A. F. Thompson, S. Aoki, Multidecadal warming of Antarctic waters. *Science* **346**, 1227–1231 (2014).
29. A. J. Payne, P. R. Holland, A. P. Shepherd, I. C. Rutt, A. Jenkins, I. Joughin, Numerical modeling of ocean-ice interactions under Pine Island Bay's ice shelf. *J. Geophys. Res. Oceans* **112**, C10019 (2007).
30. J. Suckale, J. D. Platt, T. Perol, J. R. Rice, Deformation-induced melting in the margins of the West Antarctic ice streams. *J. Geophys. Res. Earth Surf.* **119**, 1004–1025 (2014).
31. C. R. Meyer, B. M. Minchew, Temperate ice in the shear margins of the Antarctic Ice Sheet: Controlling processes and preliminary locations. *Earth Planet. Sci. Lett.* **498**, 17–26 (2018).
32. C. Raymond, K. Echelmeyer, I. M. Whillans, C. Doake, Ice Stream Shear Margins, in *The West Antarctic Ice Sheet: Behavior and Environment*, R. B. Alley, R. A. Bindschadle, Eds. (American Geophysical Union, Washington, DC, 2001), vol. 77.

33. M. A. Fahnestock, I. Joughin, T. A. Scambos, R. Kwok, W. B. Krabill, S. Gogineni, Ice-stream-related patterns of ice flow in the interior of northeast Greenland. *J. Geophys. Res. Atmos.* **106**, 34035–34045 (2001).
34. K. L. Riverman, R. B. Alley, S. Anandakrishnan, K. Christianson, N. D. Holschuh, B. Medley, A. Muto, L. E. Peters, Enhanced firn densification in high-accumulation shear margins of the NE Greenland Ice Stream. *J. Geophys. Res. Earth Surf.* **124**, 365–382 (2019).
35. I. M. Howat, C. Porter, B. E. Smith, M.-J. Noh, P. Morin, The reference elevation model of Antarctica. *Cryosphere* **13**, 665–674 (2019).
36. A. M. Le Brocq, N. Ross, J. A. Griggs, R. G. Bingham, H. F. J. Corr, F. Ferraccioli, A. Jenkins, T. A. Jordan, A. J. Payne, D. M. Rippin, M. J. Siegert, Evidence from ice shelves for channelized meltwater flow beneath the Antarctic Ice Sheet. *Nat. Geosci.* **6**, 945–948 (2013).
37. T. A. Scambos, T. M. Haran, M. A. Fahnestock, T. H. Painter, J. Bohlander, MODIS-based Mosaic of Antarctica (MOA) data sets: Continent-wide surface morphology and snow grain size. *Remote Sens. Environ.* **111**, 242–257 (2007).
38. K. E. Alley, T. A. Scambos, R. S. Anderson, H. Rajaram, A. Pope, T. M. Haran, Continent-wide estimates of Antarctic strain rates from Landsat 8-derived velocity grids. *J. Glaciol.* **64**, 321–332 (2018).

Acknowledgments
Funding: This project was funded by USGS grant 140G0118C0005, NASA grant NNX16AJ88g, NASA grant NNX16AM01G, and NSF grant 1738934. **Author contributions:** K.E.A. led the analysis, investigation, visualization, and writing of this manuscript. K.E.A. and R.B.A. led the conceptualization. All authors significantly contributed to the conceptualization and writing of the manuscript. **Competing interests:** The authors declare that they have no competing interests. **Data and materials availability:** All data needed to evaluate the conclusions in the paper are present in the paper and/or the Supplementary Materials. Additional data related to this paper may be requested from the authors.

Submitted 4 March 2019
Accepted 11 September 2019
Published 9 October 2019
10.1126/sciadv.aax2215

Citation: K. E. Alley, T. A. Scambos, R. B. Alley, N. Holschuh, Troughs developed in ice-stream shear margins precondition ice shelves for ocean-driven breakup. *Sci. Adv.* **5**, eaax2215 (2019).